

Multiple dimensions of epigenetic gene regulation in the malaria parasite *Plasmodium falciparum*

Gene regulation via histone modifications, nucleosome positioning and nuclear architecture in *P. falciparum*

Ferhat Ay^{1)*,†}, Evelien M. Bunnik^{2)†}, Nelle Varoquaux³⁾⁴⁾⁵⁾, Jean-Philippe Vert³⁾⁴⁾⁵⁾, William Stafford Noble¹⁾⁶⁾ and Karine G. Le Roch^{2)*}

Plasmodium falciparum is the most deadly human malarial parasite, responsible for an estimated 207 million cases of disease and 627,000 deaths in 2012. Recent studies reveal that the parasite actively regulates a large fraction of its genes throughout its replicative cycle inside human red blood cells and that epigenetics plays an important role in this precise gene regulation. Here, we discuss recent advances in our understanding of three aspects of epigenetic regulation in *P. falciparum*: changes in histone modifications, nucleosome occupancy and the three-dimensional genome structure. We compare these three aspects of the *P. falciparum* epigenome to those of other eukaryotes, and show that large-scale compartmentalization is particularly important in determining histone decomposition and gene regulation in *P. falciparum*. We conclude by presenting a gene regulation

model for *P. falciparum* that combines the described epigenetic factors, and by discussing the implications of this model for the future of malaria research.

Keywords:

epigenetics; gene regulation; histone modifications; malaria; nucleosome occupancy; three-dimensional genome organization; virulence genes



Additional supporting information may be found in the online version of this article at the publisher's web-site.

Introduction

The complex life cycle of *Plasmodium falciparum* includes multiple stages in both the human host and the mosquito

DOI 10.1002/bies.201400145

¹⁾ Department of Genome Sciences, University of Washington, Seattle, WA, USA

²⁾ Department of Cell Biology and Neuroscience, University of California, Riverside, CA, USA

³⁾ MINES ParisTech, PSL Research University, CBIO-Centre for Computational Biology, Fontainebleau, France

⁴⁾ Institut Curie, Paris, France

⁵⁾ U900, INSERM, Paris, France

⁶⁾ Department of Computer Science and Engineering, University of Washington, Seattle, WA, USA

[†]These authors contributed equally.

*Corresponding authors:

Ferhat Ay

E-mail: ferhatay@uw.edu

Karine G. Le Roch

E-mail: karine.leroch@ucr.edu

Abbreviations:

3C, chromatin conformation capture; **4C**, circularized chromatin conformation capture; **ApiAP2**, a family of transcription factors in *Plasmodium*; **ChIA-PET**, chromatin interaction analysis by paired-end tag sequencing; **ChIP**, chromatin immunoprecipitation; **FISH**, fluorescent in situ hybridization; **H2A**, histone H2A; **H2A.Z**, **H2B.Z**, variants of histone H2A and H2B; **H3K9ac**, histone H3 lysine 9 acetylation; **H3K(N)me3**, histone H3 lysine (N) trimethylation; **H4K20me3**, histone H4 lysine 20 trimethylation; **Hi-C**, chromatin conformation capture coupled to next-generation sequencing; **Hox**, a group of homeobox genes; **hpi**, hours post invasion; **OR**, olfactory receptors; **PfEMP1**, *Plasmodium falciparum* erythrocyte membrane protein 1; **PTM**, post-translational modification; **SHH**, sonic hedgehog gene; **TAD**, topologically associated domain; **TSS**, transcription start site; **var**, family of genes that encode PfEMP1 proteins.

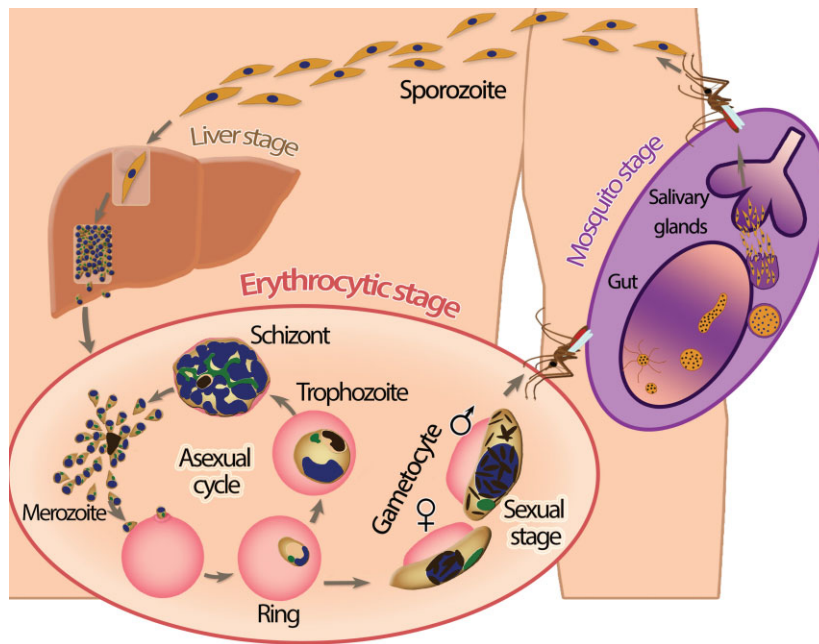


Figure 1. Overview of the *P. falciparum* life cycle.

vector (reviewed in [1]) (Fig. 1). Human infection starts with the bite of an infected female *Anopheles* mosquito, resulting in the transfer of sporozoites that quickly migrate to the liver. Inside liver cells (*hepatocytes*), these sporozoites multiply extensively over a period of approximately two weeks and are then released into the bloodstream in the form of thousands of merozoites (Fig. 1 – liver stage). During the next stage of its life cycle, the parasite replicates in red blood cells (*erythrocytes*) by means of an unusual process of cell division called *schizogony*. While the parasite progresses through three distinct developmental stages (ring, trophozoite, and schizont), it undergoes multiple rounds of nuclear replication followed by division of the multinucleated parasite into 16–32 daughter merozoites (Fig. 1 – asexual cycle). Upon bursting out of the host cell, these merozoites are released into the bloodstream and will invade new erythrocytes. During the asexual cycle, the parasite can commit to sexual development (reviewed in [2]), resulting in differentiation into a male or female gametocyte (Fig. 1 – sexual stage). The uptake of mature gametocytes by a feeding mosquito followed by the further development of the parasite in the mosquito midgut completes the *P. falciparum* life cycle (Fig. 1 – mosquito stage).

The asexual replication cycle is responsible for symptomatic disease and for the complications that are associated with severe malaria, such as anemia due to rupturing of red blood cells. In addition, severe disease can result from *cytoadherence*, the attachment of *P. falciparum*-infected erythrocytes to the smallest blood vessels, preventing clearance by the spleen and causing organ dysfunction. This cytoadherence is mediated by a family of parasite virulence proteins that are expressed on the erythrocyte surface: *Plasmodium falciparum* Erythrocyte Membrane Protein 1 (PfEMP1) [3–5]. Each *P. falciparum* parasite has approximately 60 different PfEMP1 variants encoded by *var* genes, only one of which is expressed at any time. Switching

var gene expression enables the parasite to escape from host immune responses [6, 7]. This process of antigenic variation is one example of the excellent adaptation of the parasite to survive in the human host.

The development of *P. falciparum* through the different stages of its life cycle is thought to be driven by coordinated changes in gene expression. Over the last decade, it has become clear that the parasite relies on an unusual combination of regulatory mechanisms for gene expression, and that these mechanisms are largely dependent on epigenetic processes (reviewed in [8–13]). In multicellular eukaryotes, gene expression is often mediated by transcription factors that bind to cell- or tissue-specific promoters and give rise to the expression of a subset of genes specific to that cell type or tissue [14]. However, despite extensive computational searches, relatively few transcription factors have been identified in *P. falciparum* [15, 16], only a handful of which are known to be specific to a certain stage [17]. A notable example is PfAP2-G – a member of the ApiAP2 tran-

scription factor family, which drives expression of gametocyte-specific genes and is crucial for the development of gametocytes [18, 19]. On the other hand, a relatively large number of genes are predicted to encode proteins involved in chromatin structure, mRNA decay and translation rates [16], suggesting that alternative mechanisms of gene regulation, at the epigenetic as well as post-translational levels, may be more important for gene regulation in *P. falciparum*.

Here, we focus on three important aspects of epigenetic gene regulation in *P. falciparum*, all of which are related to how DNA is packed in the nucleus (see [20–24] for articles discussing post-transcriptional regulation and see [25] for a discussion on DNA methylation, which is not well-characterized in *P. falciparum*). Similar to other eukaryotes, *P. falciparum* packages its DNA in the form of a condensed DNA–protein complex called chromatin. The basic packaging unit is a nucleosome, a stretch of approximately 147 bp of DNA wrapped around a core of eight histone proteins. Several layers of higher-order compaction of these strings of nucleosomes together create a highly structured nucleus. The organization of chromatin at both local and global levels is known to be involved in transcriptional regulation [26–29]. Local chromatin structure encompasses two main regulatory processes: the post-translational modification (PTM) of histone proteins that form nucleosomes, and nucleosome occupancy, which comprises the location, frequency, and binding strength and protein composition (i.e. variant vs. canonical histones) of nucleosomes on DNA.

At the global level, the organization of chromatin has been studied extensively, initially using gene-by-gene approaches such as immunofluorescent microscopy and fluorescent in situ hybridization (FISH) and, more recently, with chromatin conformation capture (3C)-based next-generation sequencing assays. 3C-based assays have enabled genome-wide profiling

of chromatin contacts for various organisms including human, mouse, fruit fly, budding yeast, and *P. falciparum* [30–35]. These profiles have yielded significant insights into the relationship between chromatin organization and transcription, revealing, for example, the compartmentalization of the genome into regions of transcriptionally active euchromatin and transcriptionally silent heterochromatin. Furthermore, for the haploid *P. falciparum* genome, the 3D models inferred from these contact profiles allowed the tracking of changes in nuclear organization throughout different stages of the parasite life cycle [30].

In the following sections, we provide an overview of our current understanding of chromatin organization and its role in transcriptional regulation in *P. falciparum*. We first describe various characteristics of local chromatin structure and subsequently focus on three-dimensional genome architecture. Finally, we combine these local and global views of chromatin to provide a model that explains our current understanding of the overall nuclear organization in *P. falciparum* and the role of the epigenome in regulating gene expression.

Histone modification landscape of the *P. falciparum* genome favors euchromatin

Post-translational modification of histone proteins

Histone proteins consist of a globular core structure and an N-terminal tail that protrudes from this core domain. Many amino acid residues in the core domain and in particular in the N-terminal tail can be chemically modified, producing various effects on chromatin organization (Fig. 2). In general, the addition of an acetyl group neutralizes the positive charge of histone proteins and thereby disrupts the stability of the DNA-histone interaction. This destabilization results in a more open chromatin structure and promotes a transcriptionally permissive state. On the other hand, methylations are uncharged and do not directly interfere with the interaction between histones and DNA. Rather, methylations mostly function by recruiting other effector molecules to the locus, resulting in further modifications of the chromatin.

Activating histone marks are abundant and broadly distributed

In *P. falciparum*, mass spectrometry experiments have identified at least 50 different histone PTMs, including methylation, acetylation, phosphorylation, ubiquitylation, and sumoylation [36–39]. Subsequent chromatin immunoprecipitation (ChIP) studies have given us insight into the genome-wide distribution of these histone marks in the asexual cycle (Table 1). In contrast to multicellular eukaryotes, a large proportion of the genome in *P. falciparum* is constitutively acetylated [37, 40]. An abundance of activating marks has also been observed for other unicellular organisms, such as *Saccharomyces cerevisiae* and *Tetrahymena thermophila* [41]. Inhibition of histone acetyltransferase and deacetylase activity influences the expression levels of the

majority of genes and interferes with parasite growth [42–44], indicative of the importance of acetylation for regulating transcription levels. Activating marks H3K9ac and H3K4me3 are mainly located in intergenic regions [45–47]. Highly transcribed genes carry more H3K9ac marks in their promoter [45], and this marking extends into the 5' coding region [47].

Repressive histone marks are scarce, and localized to specific regions

Typical repressive marks, in particular H3K9me3, are almost exclusively found in repressive clusters containing genes belonging to the virulence families, such as *var*, *rifin*, *stevor*, and *pfmc-2tm* [40, 46, 48, 49]. Interestingly, H3K9me3 is also present at several additional loci, including the gene encoding the gametocyte-specific transcription factor PfAP2-G [40] that is tightly repressed during the asexual cycle. Transcription start sites (TSSs) of silent *var* genes are also enriched for H3K36me3 [46], while this modification is found at equal levels inside coding regions of active and repressed *var* genes [46, 50]. H3K36me3 is present at lower levels in the rest of the genome and is enriched at the 3' end of coding regions of active *P. falciparum* genes [46], in agreement with its role in transcriptional elongation in other eukaryotes. The repressive mark H4K20me3 is also mainly present in *var* gene clusters, although its enrichment is not as strong as for H3K9me3 and H3K36me3 [46]. On the other hand, the single active *var* gene, out of ~60 family members, is enriched in active histone marks, such as H3K9ac, H3K4me3, and H4 acetylations [46, 49]. Finally, the repressive mark H3K27me3 has not been detected in the parasite [39], similar to yeast. The *P. falciparum* genome organization thus seems unusual in that a large fraction of its chromatin is continuously in a transcriptionally permissive state, while the formation of heterochromatin seems to be limited to virulence and specific sexual genes.

Histone variants and nucleosome occupancy are associated with gene expression

Relative to other eukaryotes, Plasmodium exhibits a distinctive nucleosome landscape around coding regions

Nucleosome occupancy plays an important role in regulating gene expression by allowing or restricting access of the transcription machinery to the DNA. Nucleosomes are not placed uniformly along the genome, but show a distinct distribution around coding regions [51–55]. In yeast, human and mouse, the promoter is characterized by a nucleosome-depleted region, bordered on either side by strongly positioned -1 and $+1$ nucleosomes, respectively, both of which are enriched for the variant histone H2A.Z [56–58]. The $+1$ nucleosome is located at a fixed distance relative to the TSS, although this distance varies between organisms [55]. The $+2$, $+3$, and subsequent nucleosomes form an array of nucleosomes with increasingly more fuzzy positioning toward

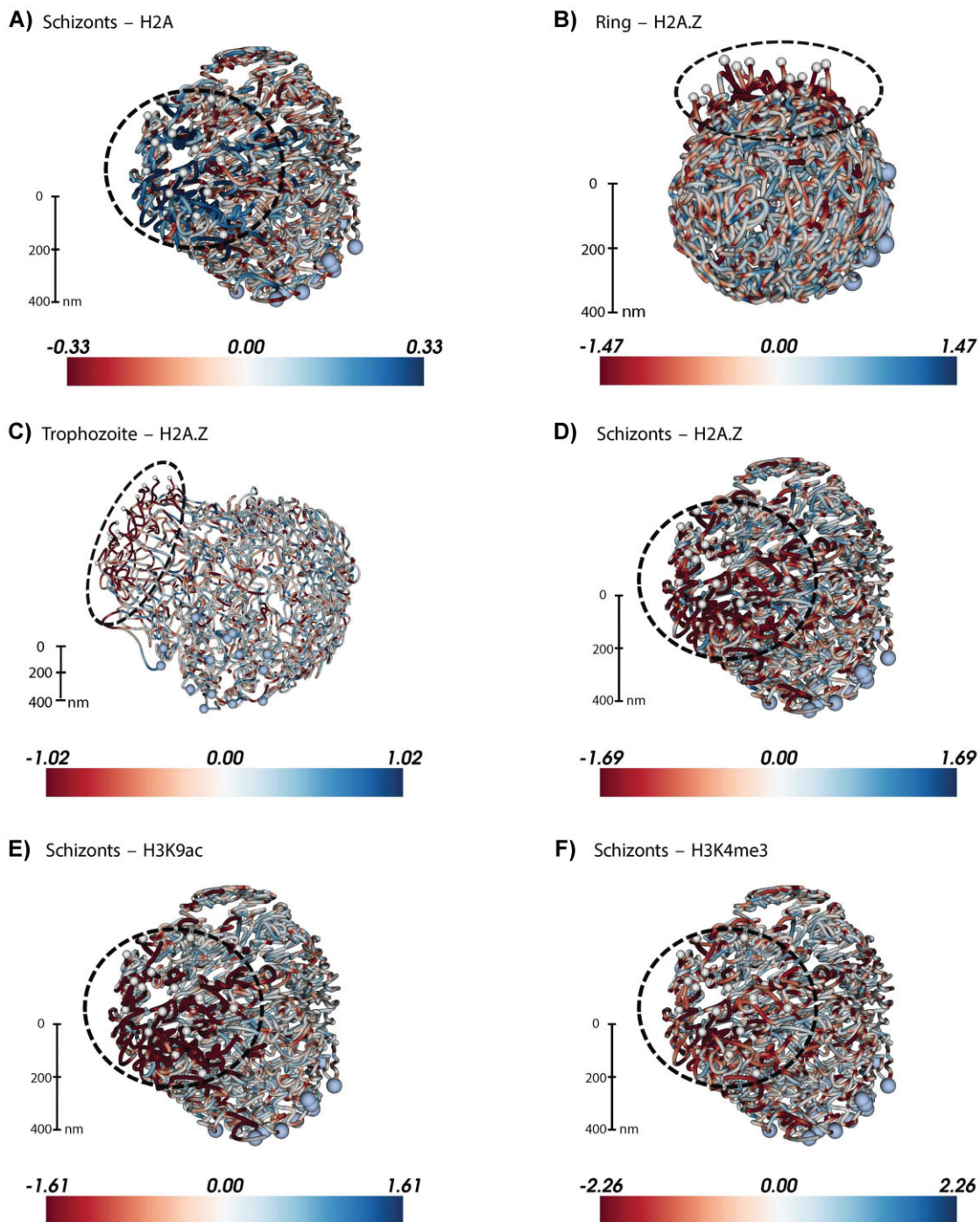


Figure 2. Large-scale depletion of the transcriptionally permissive histone variant H2A.Z and activating histone marks in the telomeric cluster visualized on the 3D *P. falciparum* genome. ChIP-seq data from Bartfai et al. [45] for four histone variants or marks were downloaded from GEO (accession number: GSE23787) and mapped to the *P. falciparum* genome (PlasmoDB v9.0) using the short read alignment mode of BWA (v0.5.9) [117] with default parameter settings. Reads were post-processed, and only the reads that map uniquely with a quality score above 30 and with at most two mismatches were retained for further analysis. Retained reads were subjected to PCR duplicate elimination and then were aggregated for each non-overlapping 5 kb bin across the *P. falciparum* genome. The number of reads for each 5 kb bin was normalized using the overall sequencing depth of the corresponding ChIP-seq library. Plotted are the log₂ ratios of sequence-depth normalized number of reads from the ChIP-seq library versus the corresponding input library (red: depletion, blue: enrichment) for **A:** H2A at 40 hours post invasion (hpi), **B:** H2A.Z at 10 hpi, **C:** H2A.Z at 30 hpi, **D:** H2A.Z at 40 hpi, **E:** H3K9ac at 40 hpi, and **F:** H3K4me3 at 40 hpi. 3D models for the ring, trophozoite and schizont stages were generated in Ay et al. [30] and were colored with ChIP-seq enrichment/depletion from 10, 20, and 40 hpi, respectively. Light blue and white spheres indicate centromeres and telomeres, respectively. The black dashed circle denotes the telomeric cluster for each stage. See Supporting information or <http://noble.gs.washington.edu/proj/plasmo-epigenetics> for the rotating 3D figure of each available ChIP-seq library.

Table 1. Overview of most-studied histone modifications and variants in *P. falciparum* and comparison of their genome-wide distribution or function in other eukaryotes

Histone PTM/variant	Other eukaryotes	<i>P. falciparum</i>
H3K4me3	Promoters of active genes [105–108]	Widely distributed in intergenic regions [45, 47]
H3K9ac	Promoters of active genes [107, 109]	Widely distributed in intergenic regions [45, 47]
H3K9me3	Silent genes [107, 108]	Repressed <i>var</i> genes [40, 48, 49]
H3K27me3	Promoters of silent/poised genes [107, 108, 110], absent in yeast [111]	Not detected [39]
H3K36me3	Enriched in pericentromeric heterochromatin [112]; transcribed regions of active genes [107, 108]	TSS of repressed <i>var</i> genes [46]; 3' end coding region active genes [46]
H4K20me3	Silencing of telomeres, transposons and long terminal repeats [108, 110]; inactive promoters [107]	Repressed <i>var</i> genes [46] and broad distribution across additional loci [40]
H2A.Z	Enriched in nucleosomes bordering active promoter (reviewed in [113, 114])	Widely distributed in intergenic regions [66, 67]
H2B.Z	Lineage-specific variants with specialized functions, for example, enriched at TSS in <i>Trypanosoma brucei</i> [68]	Widely distributed in intergenic regions [66, 67]

the 3' end of the gene. Finally, the transcription stop site is again demarcated by a strongly positioned nucleosome, followed by another nucleosome-depleted region.

Nucleosome organization in *P. falciparum* is similar to that in other eukaryotes in several respects. First, the promoter region is depleted of nucleosomes [59–61], the level of which correlates with transcriptional activity. Second, highly expressed genes have a more open chromatin organization at their core promoter than silent genes [59, 60]. However, the *P. falciparum* nucleosome landscape also exhibits a number of unusual features. Notably, the TSS is not marked by a strongly positioned +1 nucleosome; instead, the strongest nucleosomes are the first and last nucleosomes within the coding region [59, 60]. Furthermore, telomeric repeats and subtelomeric regions that contain the virulence gene families (*var*, *rifin*, etc.) have higher nucleosome occupancy levels than the bulk of the genome [59, 61, 62]. Intergenic regions, on the other hand, contain lower nucleosome levels than coding regions [59, 61–63], which is likely to be related to their extremely high AT-content (90–95%). AT-rich DNA is inherently inflexible, hampering the winding of DNA around the histone core [64, 65]. Finally, intergenic regions in *P. falciparum* are exclusively occupied by nucleosomes composed of histone variants H2A.Z and H2B.Z [66, 67], which are thought to have adopted a specialized function in *P. falciparum* to allow nucleosome assembly in these highly AT-rich regions. These histone variants are thus not restricted to promoter flanking nucleosomes but have a much broader distribution.

Nucleosome dynamics change in concordance with transcriptional activity during the asexual cycle

Another unconventional feature of nucleosome organization in *P. falciparum* is that nucleosome levels vary considerably during the asexual replication cycle, in parallel with changes in transcriptional activity [59, 63]. At the transcriptionally most active trophozoite stage, histone levels decrease by

approximately twofold [59, 63]. This nucleosome depletion occurs in a genome-wide fashion and is not restricted to genes that are expressed in the trophozoite stage. As the asexual cycle progresses into the schizont stage, nucleosomes are re-assembled, resulting in condensation of DNA as the parasites prepare for egress and invasion of a new red blood cell. Given the correlation between nucleosome density in promoter regions and gene expression levels, the dynamic nucleosome landscape in *P. falciparum* may have evolved to compensate for a paucity of specific transcription factors. Interestingly, *Trypanosoma brucei*, a parasite causing sleeping sickness in humans, has also developed an unusual nucleosome landscape, where certain combinations of canonical and variant histones mark the transcription initiation and termination sites in its genome [68]. Reminiscent of the lack of transcription factors in *P. falciparum*, transcription factors have remained elusive in *T. brucei*, indicating that these parasites may have followed parallel evolutionary pathways toward the use of the nucleosome landscape as a mechanism to regulate gene expression.

Three-dimensional conformation of the *P. falciparum* genome

Principles of nuclear organization in *P. falciparum*

It has long been known that the eukaryotic nucleus is a highly structured entity. In addition to the three-dimensional conformation of the chromatin-packaged DNA, key structural landmarks include the nuclear envelope, nuclear pores, and nucleoli. For decades, various microscopic imaging techniques have been the “go-to” tools for understanding nuclear organization and chromatin architecture in many different organisms [69–71]. In *P. falciparum*, FISH applications have been instrumental in demonstrating important characteristics of genome organization in the parasite. In particular, silent *var* genes were shown to colocalize with each other near the nuclear periphery, while the single active *var* gene is located

elsewhere [40, 72, 73]. Together with the other epigenetic mechanisms outlined above – histone modifications, histone variants and nucleosome occupancy – the non-random organization of DNA into repressive centers is believed to play a crucial role in the one-at-a-time expression of 60 genes in the *var* family. Another intriguing discovery from FISH experiments was that the ribosomal DNA loci that are distributed in a seemingly random fashion on different *P. falciparum* chromosomes show non-random colocalization in 3D [74]. A more recent study employed several ultrastructural microscopy techniques to study the distribution of nuclear pore complexes and chromatin throughout the *P. falciparum* asexual cycle [75], demonstrating a striking increase in pore density during the transcriptionally active trophozoite stage, as well as chromatin decomposition near the nuclear envelope. These changes parallel previously observed changes in transcriptional activity and nucleosome occupancy that have been discussed above [63].

Profiling of eukaryotic genome architecture using next-generation sequencing applications

Within the last decade, the field of genome architecture has been revolutionized by breakthroughs in combining next generation sequencing with molecular assays that measure proximities of DNA regions to certain nuclear landmarks (e.g. lamina and nucleolus) or to other regions in cis or trans (e.g. 4C, Hi-C, and ChIA-PET) [32, 34, 76–80] (see [81] for review). Applications of these techniques to multiple genomes including human and mouse have revealed the organizational hallmarks of genome architecture. These include localization of gene-rich regions near the nuclear center and heterochromatin near the nuclear lamina [77], colocalization of ribosomal DNA loci near nucleoli [78], and megabase-scale open/closed chromatin compartments [34]. In addition, these two mammalian genomes are partitioned into megabase-sized topologically associated domains (TADs) that are enriched for

interactions within but not across domains, and are separated from each other by insulator proteins [31, 82, 83] (see [28] for review). Finally, these studies have provided us with examples of cell type-specific chromatin loops bringing distal regulatory elements into close 3D proximity. Long-range chromatin loops that play regulatory roles in gene expression include *Hox* cluster silencing [84, 85], control of *SHH* gene by an enhancer that is located 1 Mb away in human [86] and a validated set of cell type-specific enhancers in mouse [87].

Profiling of *P. falciparum* genome architecture during the asexual cycle

As is the case for many other next generation sequencing-based assays, application of these genome architecture assays has been challenging for the AT-rich genome of *P. falciparum*. However, within the last year, two groups have published their results using Hi-C, one profiling the genome architecture of different *P. falciparum* strains [33] and the other modeling the 3D structure of *P. falciparum*-3D7 at three key stages during its asexual replication cycle within human red blood cells [30]. These studies revealed key characteristics of *P. falciparum* genome structure (Table 2), including colocalization of centromeres, colocalization of telomeres near the nuclear periphery, colocalization of both internal and subtelomeric virulence gene clusters near the telomeres, colocalization of rDNA loci that are active in ring stage parasites, and maintenance of chromosomes territories (see Ay et al. [30] for details). Furthermore, Hi-C profiles from Ay et al. exhibit different polymer behavior in the most transcriptionally active trophozoite stage compared to the other two stages, suggesting a link between overall chromatin compaction and transcriptional activity. The degree of telomere colocalization and the repressive effect of the telomeric compartment is also most pronounced in this trophozoite stage, suggesting a strict compartmentalization to segregate genes that need to be repressed from the rest.

Table 2. Summary of organizational features of *P. falciparum* nucleus and genome at three distinct stages during asexual parasite replication in human red blood cells (asexual cycle)

Feature	Ring	Trophozoite	Schizont
Nuclear size	Small (~700 nm diameter) [75, 115]	Large (~1,700 nm diameter) [75, 115]	Small (~850 nm diameter) [75, 115]
Nuclear pores	Few (3–7), clustered together [75]	Many (12–58), uniformly distributed [75]	Few per daughter nucleus (2–6), clustered together [75]
Nucleosome occupancy	High [59, 63]	Low [59, 63]	High [59, 63]
Chromatin compaction	Compact [30, 59, 63, 75]	Open [30, 59, 63, 75]	Compact [30, 59, 63, 75]
Chromosome territories	Conflicting reports (absent [33] vs. present [30])	Partially lost [30]	Present [30]
Centromere locations	Conflicting reports (colocalized [30] vs. dispersed [33, 116])	Colocalized [30, 116]	Colocalized [30, 116]
Telomere locations	Colocalized near periphery [30, 72]	Colocalized near periphery [30, 72]	Colocalized near periphery [30, 72]
Virulence gene locations	Colocalized [33] near periphery [30, 40, 72]	Colocalized near periphery [30, 40, 72]	Colocalized near periphery [30, 40, 72]
rDNA gene locations	Conflicting reports (all loci clustered [74] vs. strong clustering of only active loci [30, 33])	Conflicting reports (dispersed [74] vs. weak clustering of only active loci [30])	Conflicting reports (dispersed [74] vs. weak clustering of only active loci [30])

Finally, both the Hi-C contact maps and the 3D models inferred from them suggest a tight correlation between the 3D location of a gene and its expression. Gene pairs located nearby in 3D have significantly higher expression correlation compared to other pairs, even after discarding intra-chromosomal pairs that would be biased by their genomic distance in 1D [30]. Overall, these observations suggest that *P. falciparum* chromatin is highly structured at the large scale and that this structure provides a potential epigenetic mechanism to regulate gene expression.

The folded chromosome structure seen in *P. falciparum* is similar to what has been observed in budding and fission yeast [32, 88]. However, chromosome looping to achieve localization of *var* genes in repressive perinuclear compartments results in a more complex three-dimensional organization of the *P. falciparum* genome compared to yeast, even though these organisms have similarly sized genomes [30]. Interestingly, the clonal *var* gene expression and clustering of all remaining *var* genes in repressive heterochromatin is strikingly similar to the epigenetic signature of the ~1,400 olfactory receptor genes in the mouse, all except one of which are located in heterochromatic foci enriched for H3K9me3 and H4K20me3, resulting in monogenic and monoallelic expression [89, 90]. In comparison to human, mouse, and fly genomes, the *P. falciparum* genome organization is relatively simple and does not display TADs. The nuclear architecture in *P. falciparum* thus exploits features from both unicellular and multicellular organisms. Even though the parasite is a unicellular organism throughout its entire life cycle, it adopts drastically different forms during the various life cycle stages to be able to survive in a variety of cells in both the human and the mosquito host. The regulation of life cycle progression and cell differentiation is therefore likely to be more constrained and complex than for most unicellular organisms. From an evolutionary standpoint, this may explain why the parasite has developed such complex nuclear architecture relative to the size of its genome.

A combined model of epigenetic gene regulation in *P. falciparum*

Nuclear organization and gene regulation

The epigenetic makeup of the *P. falciparum* genome, as outlined above, points toward a binary nuclear organization, with the majority of the genome present in the form of euchromatin, while a limited number of genes are organized into strongly repressed heterochromatin. This heterochromatin is localized at the nuclear periphery and is characterized by high nucleosome density (Fig. 2A), the presence of repressive histone marks H3K9me3, H3K36me3, and H4K20me3 (Fig. 3A–C), and the absence of the transcription-associated histone variant H2A.Z (Fig. 2B–D) and histone marks H3K9ac (Fig. 2E), and H3K4me3 (Figs. 2F and 3D). It was recently demonstrated that heterochromatin protein 1 (HP1) and *P. falciparum* histone deacetylase 2 (PfHda2) are both essential for maintaining heterochromatic regions [91, 92]. Depletion of either HP1 or PfHda2 resulted in an arrest of parasite development at the trophozoite stage and a loss of *var* gene repression. In addition,

an increase in the number of parasites differentiating into gametocytes was observed, indicating that the gametocyte transcription factor locus *pfap2-g* is also under strict epigenetic control. The remaining euchromatic fraction of the genome has several notable features, including perinuclear compartments containing the active *var* gene or active rDNA genes (Fig. 4A). In addition, clustering of silent genes that are specific to other stages of the parasite's life cycle [30] suggests the presence of small heterochromatic islands, as observed at the trophozoite stage by advanced transmission and scanning electron microscopy [75].

Remodeling of the nuclear organization during the asexual cycle

Microarray and RNA-seq studies have shown that 70–80% of all genes are expressed in the asexual replication cycle, in particular during the trophozoite stage [24, 93, 94]. During the 48-hour cycle, the nucleus and chromatin are drastically remodeled to facilitate this high transcriptional activity (Fig. 4B and Table 2). First, the nucleus expands in size [75], which can also be readily observed in microscopy images of Giemsa stained parasites [30]. Second, the number of nuclear pores increases greatly, from 3–7 clustered pores in the ring stage to 12–58 pores that are uniformly distributed around the nucleus in the trophozoite stage [75]. Third, in line with the increased nuclear volume, the chromatin opens up [30, 75], accompanied by removal of nucleosomes [59, 63] and increased intermingling of chromosomes [30]. Despite these large-scale nuclear dynamics, the centromeres, telomeres and repressed *var* genes remain clustered. The correlation of nucleosome density of gene promoters with transcriptional activity of individual genes suggests that local chromatin organization may play an important role in regulating the level of gene expression [59]. The transitioning of the parasite from the trophozoite stage to the schizont stage is characterized by a reversion of nuclear changes, including reassembly of nucleosomes and re-establishment of chromosomal territories, which results in recompaction of the genome. Finally, during DNA replication, the nucleus divides into multiple small daughter nuclei, each with a small number of the nuclear pores, i.e. those that were present in the original nucleus [75].

Outstanding questions

Does the nucleus harbor one or more repressive centers near the periphery?

Whether heterochromatin containing silent *var* genes is organized into a single large repressive center or is divided over a small number of perinuclear foci remains a topic of debate. FISH images visualizing the location of telomere-associated repeat elements or *var* gene promoters typically show 2–6 foci distributed around the nucleus [40, 72, 73, 95]. On the other hand, single foci were observed by immunofluorescence microscopy for H3K9me3, H3K36me3, and heterochromatin protein 1 [50, 96], all of which are strongly

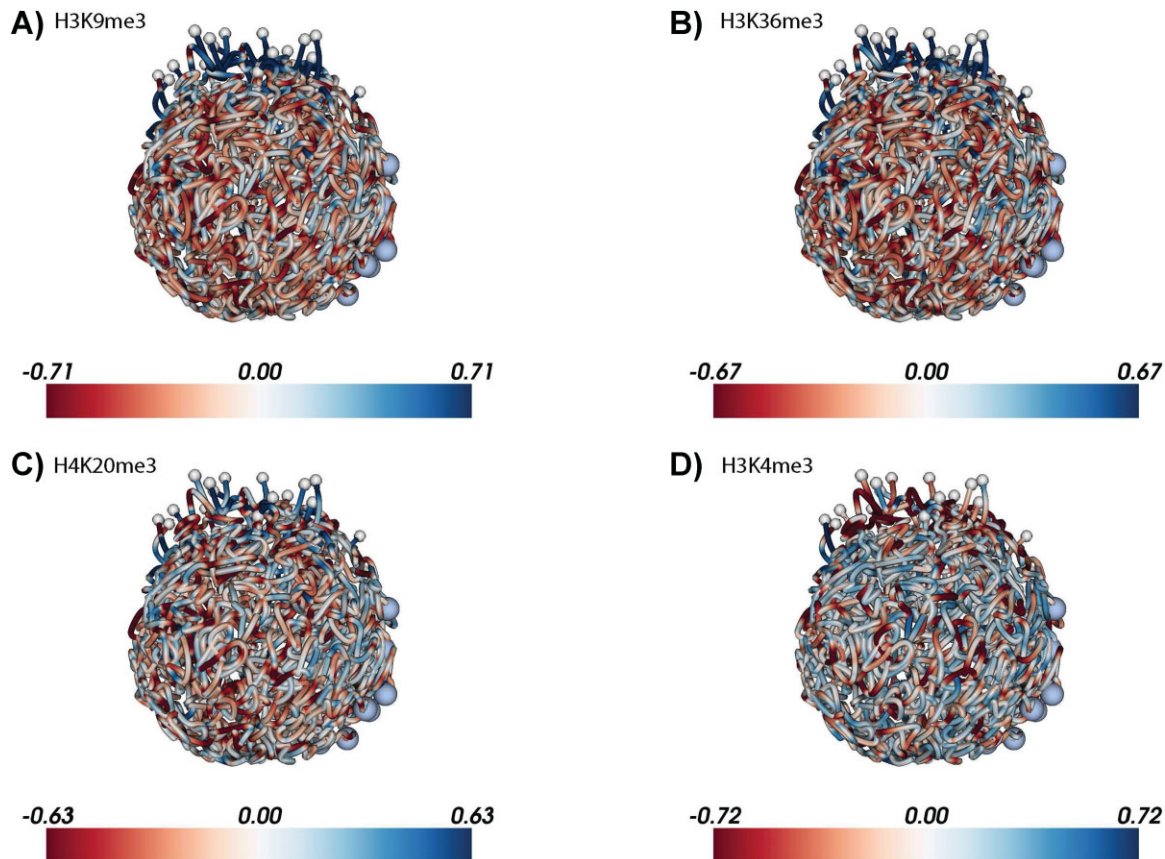


Figure 3. Enrichment of repressive histone marks in the telomeric cluster visualized on the 3D *P. falciparum* genome at the ring stage. ChIP-seq data from Jiang et al. [46] for five histone marks were downloaded from SRA (accession number: SRP022761) and processed as described in the caption of Figure 2. Due to lack of input libraries from this publication, the input libraries from Bartfai et al. at different time points were pooled into one aggregated input library which was then used for normalization of each Jiang et al. ChIP-seq library. Similar to Figure 2, log₂ ratios of ChIP-seq versus input were plotted for **A:** H3K9me₃, **B:** H3K36me₃, **C:** H4K20me₃, and **D:** H3K4me₃ at 18 hpi. The 3D model for the ring stage from Ay et al. [30] was used to visualize enrichment/depletion of each histone mark. See Supporting Information or <http://noble.gs.washington.edu/proj/plasmo-epigenetics> for the rotating 3D figure of each available ChIP-seq library.

associated with the repressed *var* genes. In addition, the Hi-C derived three-dimensional models of the *P. falciparum* genome showed strong clustering of centromeres and telomeres [30] (Fig. 4A), a chromosome configuration that has been observed in other organisms [32, 88, 97]. These models suggested the organization of subtelomeric *var* genes into a single cluster at the nuclear perimeter. Such organization, even though seemingly contradicting the FISH data, may be due to aggregation across a large population of cells for Hi-C experiments. If each *var* gene cluster is randomly located in one of multiple repressive clusters in each cell, then the aggregate signal would suggest colocalization of all *var* genes. However, it may conceivably be beneficial to locate all repressed genes in close proximity of each other to regulate

the expression of a single *var* gene and the tight repression of all remaining family members. Additional experiments will be necessary to unravel the precise mechanisms by which *var* gene expression is controlled, by further dissecting the effect of gene localization, nuclear architecture, and gene-to-gene communication on this process. In particular, Hi-C experiments on single cells would likely provide significant insight into the localization of active and repressed *var* genes, as well as the extent of cell-to-cell variability.

Could the mediators of epigenetic control and nuclear remodeling be the next drug targets for malaria?

Drastic remodeling of the nucleus and chromatin are likely to be driving forces behind the wave of transcriptional activity during the trophozoite stage. Components involved in these dynamic processes may thus be promising targets for antimalarial drugs. Future research should therefore focus on understanding the molecular mechanisms involved in chromatin and nuclear remodeling. For example, very little is known about proteins and enzymes that regulate the formation of heterochromatin and the global nuclear architecture, with the exception of the role of HP1 in maintaining repressive perinuclear chromatin containing the *var* genes and the *pfap2-g* locus. A multitude of such proteins has been identified in other organisms, most notably RNA polymerase III-associated factor (TFIIIC), cohesin and

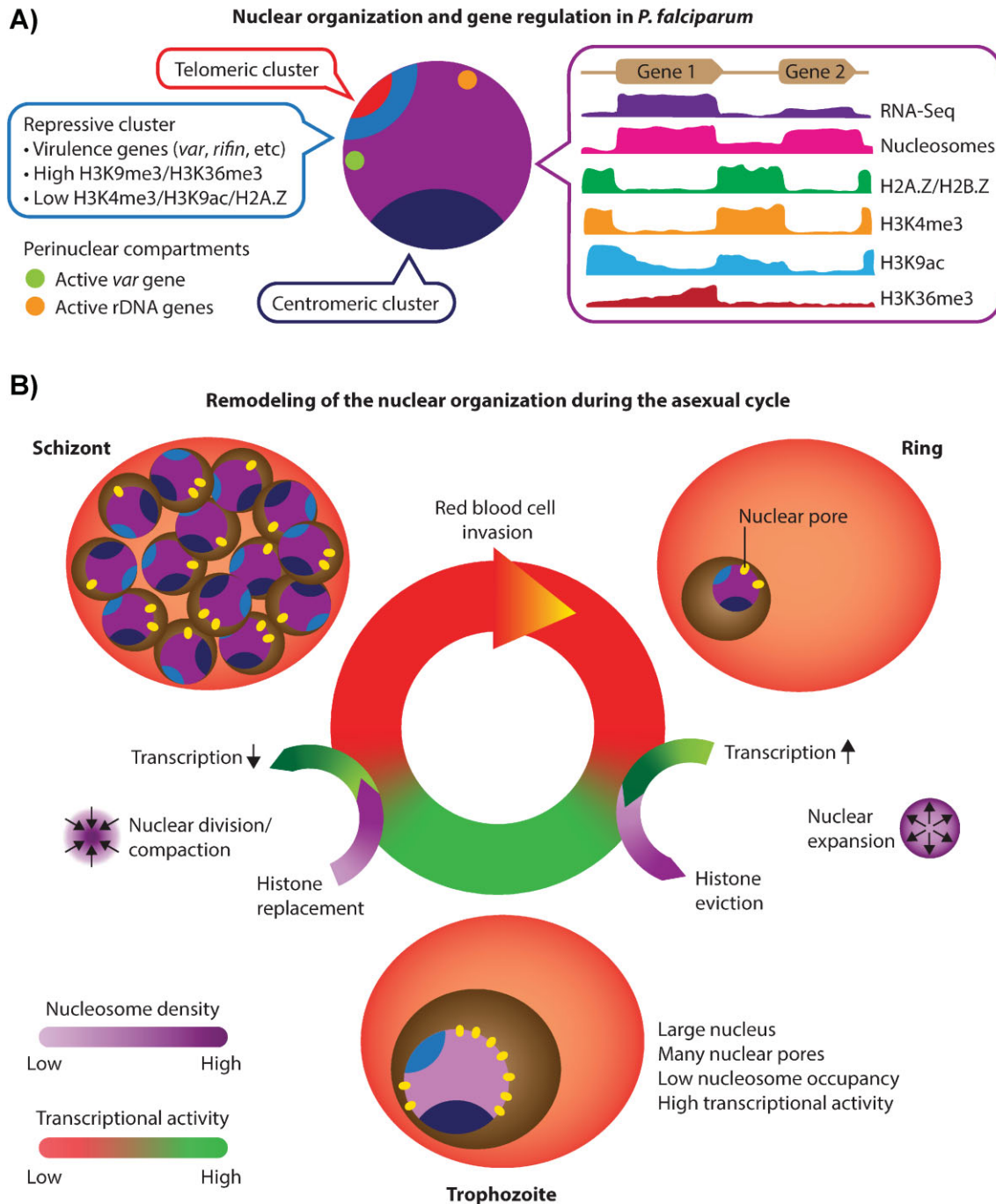


Figure 4. Model for *P. falciparum* epigenetic gene regulation. **A:** Nuclear organization and gene regulation in *P. falciparum*. Centromeric (dark blue) and telomeric (red) clusters are localized at the nuclear periphery. Subtelomeric virulence genes (blue) are anchored to the nuclear perimeter and cluster with internally located *var* genes in repressive center(s), characterized by repressive histone marks H3K9me3 and H3K36me3. The single active *var* gene (green) is located in a perinuclear compartment away from the repressive center(s). In addition, active rDNA genes (orange) also cluster at the nuclear periphery. The remaining genome (purple) is largely present in an open, euchromatic state with a number of notable features. (i) Nucleosome levels are high in genic and lower in intergenic regions, while gene expression correlates with nucleosome density at the transcription start site. (ii) Intergenic regions are bound by nucleosomes containing histone variants H2A.Z and H2B.Z. (iii) Intergenic regions contain H3K4me3, the level of which does not influence transcriptional activity. (iv) H3K9ac is mainly found in intergenic regions and extends into 5' ends of coding regions, with highly expressed genes showing higher levels of H3K9ac. (v) Active genes are marked with H3K36me3 toward their 3' end. **B:** Remodeling of the nuclear organization during the asexual cycle. Extensive remodeling of the nucleus takes place as the parasite progresses through the ring, trophozoite and schizont stages. In the transition from the relatively inert ring stage to the transcriptionally active trophozoite stage, the size of the nucleus and the number of nuclear pores increase, accompanied by a decrease in genome-wide nucleosome levels, resulting in an open chromatin structure that allows high transcription rates. In the schizont stage, the nucleus divides and recompacts, histones are re-assembled and transcription is shut-down, to facilitate egress of the parasites' daughter cells and invasion of new red blood cells.

CCCTC binding factor (CTCF) (reviewed in [98]), that are likely to have homologues in *P. falciparum*. Other potential drug targets include key components involved in expansion of the nuclear membrane and chromatin remodeling enzymes that regulate the global nucleosome eviction and re-assembly during the trophozoite and schizont stages. Analysis of chromatin-associated proteins by proteomics-based approaches will likely identify many candidates that may be involved in these processes. In addition, the application of novel genetic engineering tools in *P. falciparum*, such as the CRISPR/Cas9 system [99–101], may enable us to study the effect of gene deletion or translocation on genome structure to better understand the determinants of nuclear architecture.

Are the epigenetic control mechanisms similar in other stages of *P. falciparum* life cycle and in other parasites?

The epigenetic regulation model we present here is based on profiles taken during the asexual replication cycle. During this phase of the parasite's life cycle, the genome seems to be largely shaped by the strict one-at-a-time expression of the *var* genes. The absence of *var* gene expression in all other parasite stages may have a large impact on chromatin organization. In addition, while some genes may be constitutively expressed during the parasite's life cycle, others may be silenced or activated in these alternative and highly variable stages, ranging from the male and female gametocyte, via the diploid zygote in the mosquito midgut, to the haploid sporozoite. Therefore, we expect generating genome-wide profiles of histone modifications, nucleosome landscape and three-dimensional architecture during these other parasite stages to be of great interest to further explore the epigenetic regulatory mechanisms in *P. falciparum*.

Furthermore, we know very little about the role of epigenetic control in transcriptional regulation in other *Plasmodium* species. *P. vivax*, for example, has a much lower AT-content (on average 57%), which is likely to influence the binding kinetics and preferences of nucleosomes. In addition, *P. vivax* expresses a large proportion of its gene family encoding for variant surface proteins (*vir*) during the blood stage, whereas *P. falciparum* expresses only one out of its 60 *var* genes in this stage [102, 103]. In *P. vivax* the absence of clonal expression, as seen for the *var* family in *P. falciparum*, may reduce the requirements for strictly repressive heterochromatin. Therefore, determining the nucleosome landscape, the location of histone modifications and the three-dimensional structure of the *P. vivax* genome will be extremely informative for our understanding of commonalities and differences between epigenetic gene regulation in these two parasites, especially pertaining to regulation of virulence genes.

Conclusions and prospects

An increasing amount of data highlights the importance of epigenetic mechanisms in regulating gene expression in *P. falciparum* and other eukaryotes, including human and

mouse [30–35]. Here, we have discussed multiple layers of epigenetic control, including histone modifications, nucleosome occupancy, histone variants and genome architecture, which are involved in the precise gene regulation during the asexual replication cycle of the malaria parasite, *P. falciparum*. We summarized the current understanding of the interplay among these different layers and how these layers shape the overall nuclear organization and connect with overall transcriptional activity and to the one-at-a-time expression of *var* genes.

Better characterization of epigenetic regulation in *P. falciparum* will stimulate interest in several exciting directions in malaria research. Further studies into the establishment and maintenance of strong repressive compartments in the nucleus may reveal the underlying regulatory mechanisms and lead to the identification of proteins involved in this process. Disrupting the function of proteins responsible for maintaining heterochromatin, such as HP1 [91], could be an effective strategy to block parasite replication during the asexual cycle. Another important event in the malaria life cycle is gametocytogenesis, which was recently shown to be driven by the transcription factor PfAP2-G [18, 19]. It would be interesting to fully characterize the epigenetic factors, such as genome architecture, that help PfAP2-G target and regulate gametocyte-specific genes. In addition to layers of epigenetic regulation that we have focused on here, post-transcriptional and translational controls are likely to be involved in the timing of protein expression [22–24, 104]. Increased insight into these regulatory processes would significantly advance our understanding of parasite biology and could facilitate major breakthroughs in our fight against malaria.

Acknowledgments

This study was financially supported by a Computing Research Association CIFellows award (NSF award CIF 1136996 to F.A.), the Human Frontier Science Program (grant LT000507/2011-L to E.M.B.), the National Institutes of Health (grants R01 AI85077-04 to K.L.R. and R01 AI106775-02 to W.S.N./K.L.R.), the European Research Council (grant SMAC-ERC-280032 to J.P.V.), the European Commission (grant HEALTH-F5-2012-305626 to J.P.V./N.V.) and the French National Research Agency (grant ANR-11-BINF-0001 to J.P.V./N.V.).

The authors have declared no conflict of interest.

References

1. Greenwood BM, Fidock DA, Kyle DE, Kappe SH, et al. 2008. Malaria: progress, perils, and prospects for eradication. *J Clin Invest* **118**: 1266–76.
2. Baker DA. 2010. Malaria gametocytogenesis. *Mol Biochem Parasitol* **172**: 57–65.
3. Baruch DI, Pasloske BL, Singh HB, Bi X, et al. 1995. Cloning the *P. falciparum* gene encoding PfEMP1, a malarial variant antigen and adherence receptor on the surface of parasitized human erythrocytes. *Cell* **82**: 77–87.
4. Smith JD, Chitnis CE, Craig AG, Roberts DJ, et al. 1995. Switches in expression of *Plasmodium falciparum* *var* genes correlate with changes in antigenic and cytoadherent phenotypes of infected erythrocytes. *Cell* **82**: 101–10.

5. **Su XZ, Heatwole VM, Wertheimer SP, Guinet F**, et al. 1995. The large diverse gene family var encodes proteins involved in cytoadherence and antigenic variation of *Plasmodium falciparum*-infected erythrocytes. *Cell* **82**: 89–100.
6. **Bull PC, Lowe BS, Kortok M, Molyneux CS**, et al. 1998. Parasite antigens on the infected red cell surface are targets for naturally acquired immunity to malaria. *Nat Med* **4**: 358–60.
7. **Roberts DJ, Craig AG, Berendt AR, Pinches R**, et al. 1992. Rapid switching to multiple antigenic and adhesive phenotypes in malaria. *Nature* **357**: 689–92.
8. **Cui L, Miao J**. 2010. Chromatin-mediated epigenetic regulation in the malaria parasite *Plasmodium falciparum*. *Eukaryot Cell* **9**: 1138–49.
9. **Duffy MF, Selvarajah SA, Josling GA, Petter M**. 2012. The role of chromatin in *Plasmodium* gene expression. *Cell Microbiol* **14**: 819–28.
10. **Hoeijmakers WA, Stunnenberg HG, Bartfai R**. 2012. Placing the *Plasmodium falciparum* epigenome on the map. *Trends Parasitol* **28**: 486–95.
11. **Horrocks P, Wong E, Russell K, Emes RD**. 2009. Control of gene expression in *Plasmodium falciparum* – ten years on. *Mol Biochem Parasitol* **164**: 9–25.
12. **Deutsch K, Duraisingh M, Dzikowski R, Gunasekera A**, et al. 2007. Mechanisms of gene regulation in *Plasmodium*. *Am J Trop Med Hyg* **77**: 201–8.
13. **Voss TS, Bozdech Z, Bartfai R**. 2014. Epigenetic memory takes center stage in the survival strategy of malaria parasites. *Curr Opin Microbiol* **20**: 88–95.
14. **Consortium EP**. 2012. An integrated encyclopedia of DNA elements in the human genome. *Nature* **489**: 57–74.
15. **Balaji S, Babu MM, Iyer LM, Aravind L**. 2005. Discovery of the principal specific transcription factors of Apicomplexa and their implication for the evolution of the AP2-integrase DNA binding domains. *Nucleic Acids Res* **33**: 3994–4006.
16. **Coulson RM, Hall N, Ouzounis CA**. 2004. Comparative genomics of transcriptional control in the human malaria parasite *Plasmodium falciparum*. *Genome Res* **14**: 1548–54.
17. **Campbell TL, De Silva EK, Olszewski KL, Elemento O**, et al. 2010. Identification and genome-wide prediction of DNA binding specificities for the ApiAP2 family of regulators from the malaria parasite. *PLoS Pathog* **6**: e1001165.
18. **Kafsack BF, Rovira-Graells N, Clark TG, Bancells C**, et al. 2014. A transcriptional switch underlies commitment to sexual development in malaria parasites. *Nature* **507**: 248–52.
19. **Sinha A, Hughes KR, Modrzynska KK, Otto TD**, et al. 2014. A cascade of DNA-binding proteins for sexual commitment and development in *Plasmodium*. *Nature* **507**: 253–7.
20. **Chung DW, Pons N, Cervantes S, Le Roch KG**. 2009. Post-translational modifications in *Plasmodium*: more than you think! *Mol Biochem Parasitol* **168**: 123–34.
21. **Le Roch KG, Chung DW, Pons N**. 2012. Genomics and integrated systems biology in *Plasmodium falciparum*: a path to malaria control and eradication. *Parasite Immunol* **34**: 50–60.
22. **Suvorova ES, White MW**. 2014. Transcript maturation in Apicomplexan parasites. *Curr Opin Microbiol* **20C**: 82–7.
23. **Kramer S**. 2014. RNA in development: how ribonucleoprotein granules regulate the life cycles of pathogenic protozoa. *Wiley Interdiscip Rev RNA* **5**: 263–84.
24. **Bunnik EM, Chung DW, Hamilton M, Pons N**, et al. 2013. Polysome profiling reveals translational control of gene expression in the human malaria parasite *Plasmodium falciparum*. *Genome Biol* **14**: R128.
25. **Pons N, Fu L, Harris EY, Zhang J**, et al. 2013. Genome-wide mapping of DNA methylation in the human malaria parasite *Plasmodium falciparum*. *Cell Host Microbe* **14**: 696–706.
26. **Jenuwein T, Allis CD**. 2001. Translating the histone code. *Science* **293**: 1074–80.
27. **Zentner GE, Henikoff S**. 2013. Regulation of nucleosome dynamics by histone modifications. *Nat Struct Mol Biol* **20**: 259–66.
28. **Nora EP, Dekker J, Heard E**. 2013. Segmental folding of chromosomes: a basis for structural and regulatory chromosomal neighborhoods? *BioEssays* **35**: 818–28.
29. **Belmont AS**. 2014. Large-scale chromatin organization: the good, the surprising, and the still perplexing. *Curr Opin Cell Biol* **26**: 69–78.
30. **Ay F, Bunnik EM, Varoquaux N, Bol SM**, et al. 2014. Three-dimensional modeling of the *P. falciparum* genome during the erythrocytic cycle reveals a strong connection between genome architecture and gene expression. *Genome Res* **24**: 974–88.
31. **Dixon JR, Selvaraj S, Yue F, Kim A**, et al. 2012. Topological domains in mammalian genomes identified by analysis of chromatin interactions. *Nature* **485**: 376–80.
32. **Duan Z, Andronescu M, Schutz K, Mcllwain S**, et al. 2010. A three-dimensional model of the yeast genome. *Nature* **465**: 363–7.
33. **Lemieux JE, Kyes SA, Otto TD, Feller AI**, et al. 2013. Genome-wide profiling of chromosome interactions in *Plasmodium falciparum* characterizes nuclear architecture and reconfigurations associated with antigenic variation. *Mol Microbiol* **90**: 519–37.
34. **Lieberman-Aiden E, van Berkum NL, Williams L, Imakaev M**, et al. 2009. Comprehensive mapping of long-range interactions reveals folding principles of the human genome. *Science* **326**: 289–93.
35. **Sexton T, Yaffe E, Kenigsberg E, Bantignies F**, et al. 2012. Three-dimensional folding and functional organization principles of the *Drosophila* genome. *Cell* **148**: 458–72.
36. **Lasonder E, Trecek M, Alam M, Tobin AB**. 2012. Insights into the *Plasmodium falciparum* schizont phospho-proteome. *Microbes Infect* **14**: 811–9.
37. **Miao J, Fan Q, Cui L, Li J**. 2006. The malaria parasite *Plasmodium falciparum* histones: organization, expression, and acetylation. *Gene* **369**: 53–65.
38. **Trecek M, Sanders JL, Elias JE, Boothroyd JC**. 2011. The phosphoproteomes of *Plasmodium falciparum* and *Toxoplasma gondii* reveal unusual adaptations within and beyond the parasites' boundaries. *Cell Host Microbe* **10**: 410–9.
39. **Trelle MB, Salcedo-Amaya AM, Cohen AM, Stunnenberg HG**, et al. 2009. Global histone analysis by mass spectrometry reveals a high content of acetylated lysine residues in the malaria parasite *Plasmodium falciparum*. *J Proteome Res* **8**: 3439–50.
40. **Lopez-Rubio JJ, Mancio-Silva L, Scherf A**. 2009. Genome-wide analysis of heterochromatin associates clonally variant gene regulation with perinuclear repressive centers in malaria parasites. *Cell Host Microbe* **5**: 179–90.
41. **Garcia BA, Hake SB, Diaz RL, Kauer M**, et al. 2007. Organismal differences in post-translational modifications in histones H3 and H4. *J Biol Chem* **282**: 7641–55.
42. **Cui L, Miao J, Furuya T, Fan Q**, et al. 2008. Histone acetyltransferase inhibitor anacardic acid causes changes in global gene expression during in vitro *Plasmodium falciparum* development. *Eukaryot Cell* **7**: 1200–10.
43. **Cui L, Miao J, Cui L**. 2007. Cytotoxic effect of curcumin on malaria parasite *Plasmodium falciparum*: inhibition of histone acetylation and generation of reactive oxygen species. *Antimicrob Agents Chemother* **51**: 488–94.
44. **Chaal BK, Gupta AP, Wastuwidyaningtyas BD, Luah YH**, et al. 2010. Histone deacetylases play a major role in the transcriptional regulation of the *Plasmodium falciparum* life cycle. *PLoS Pathog* **6**: e1000737.
45. **Bartfai R, Hoeijmakers WA, Salcedo-Amaya AM, Smits AH**, et al. 2010. H2A.Z. demarcates intergenic regions of the *Plasmodium falciparum* epigenome that are dynamically marked by H3K9ac and H3K4me3. *PLoS Path* **6**: e1001223.
46. **Jiang L, Mu J, Zhang Q, Ni T**, et al. 2013. PfSETvs methylation of histone H3K36 represses virulence genes in *Plasmodium falciparum*. *Nature* **499**: 223–7.
47. **Salcedo-Amaya AM, van Driel MA, Alako BT, Trelle MB**, et al. 2009. Dynamic histone H3 epigenome marking during the intraerythrocytic cycle of *Plasmodium falciparum*. *Proc Natl Acad Sci USA* **106**: 9655–60.
48. **Chookajorn T, Dzikowski R, Frank M, Li F**, et al. 2007. Epigenetic memory at malaria virulence genes. *Proc Natl Acad Sci USA* **104**: 899–02.
49. **Lopez-Rubio JJ, Gontijo AM, Nunes MC, Issar N**, et al. 2007. 5' flanking region of var genes nucleate histone modification patterns linked to phenotypic inheritance of virulence traits in malaria parasites. *Mol Microbiol* **66**: 1296–305.
50. **Ukaegbu UE, Kishore SP, Kwiatkowski DL, Pandarinath C**, et al. 2014. Recruitment of PfSET2 by RNA polymerase II to variant antigen encoding loci contributes to antigenic variation in *P. falciparum*. *PLoS Pathog* **10**: e1003854.
51. **Brogaard K, Xi L, Wang JP, Widom J**. 2012. A map of nucleosome positions in yeast at base-pair resolution. *Nature* **486**: 496–501.
52. **Buenrostro JD, Araya CL, Chircus LM, Layton CJ**, et al. 2014. Quantitative analysis of RNA-protein interactions on a massively parallel array reveals biophysical and evolutionary landscapes. *Nat Biotechnol* **32**: 562–8.
53. **Jansen A, Verstrepen KJ**. 2011. Nucleosome positioning in *Saccharomyces cerevisiae*. *Microbiol Mol Biol Rev* **75**: 301–20.

54. Lee W, Tillo D, Bray N, Morse RH, et al. 2007. A high-resolution atlas of nucleosome occupancy in yeast. *Nat Genet* **39**: 1235–44.
55. Mavrich TN, Jiang C, Ioshikhes IP, Li X, et al. 2008. Nucleosome organization in the *Drosophila* genome. *Nature* **453**: 358–62.
56. Raisner RM, Hartley PD, Meneghini MD, Bao MZ, et al. 2005. Histone variant H2A.Z. marks the 5' ends of both active and inactive genes in euchromatin. *Cell* **123**: 233–48.
57. Guillemette B, Bataille AR, Gevry N, Adam M, et al. 2005. Variant histone H2A.Z. is globally localized to the promoters of inactive yeast genes and regulates nucleosome positioning. *PLoS Biol* **3**: e384.
58. Tolstorukov MY, Kharchenko PV, Goldman JA, Kingston RE, et al. 2009. Comparative analysis of H2A.Z. nucleosome organization in the human and yeast genomes. *Genome Res* **19**: 967–77.
59. Bunnik EM, Polishko A, Prudhomme J, Ponts N, et al. 2014. DNA-encoded nucleosome occupancy is associated with transcription levels in the human malaria parasite *Plasmodium falciparum*. *BMC Genomics* **15**: 347.
60. Ponts N, Harris EY, Lonardi S, Le Roch KG. 2011. Nucleosome occupancy at transcription start sites in the human malaria parasite: a hard-wired evolution of virulence? *Infect Genet Evol* **11**: 716–24.
61. Westenberger SJ, Cui L, Dharia N, Winzeler E. 2009. Genome-wide nucleosome mapping of *Plasmodium falciparum* reveals histone-rich coding and histone-poor intergenic regions and chromatin remodeling of core and subtelomeric genes. *BMC Genomics* **10**: 610.
62. Segal E, Fondufe-Mittendorf Y, Chen L, Thastrom A, et al. 2006. A genomic code for nucleosome positioning. *Nature* **442**: 772–8.
63. Ponts N, Harris EY, Prudhomme J, Wick I, et al. 2010. Nucleosome landscape and control of transcription in the human malaria parasite. *Genome Res* **20**: 228–38.
64. Tillo D, Hughes TR. 2009. G+C content dominates intrinsic nucleosome occupancy. *BMC Bioinformatics* **10**: 442.
65. Segal E, Widom J. 2009. Poly(dA:dT) tracts: major determinants of nucleosome organization. *Curr Opin Struct Biol* **19**: 65–71.
66. Hoeijmakers WA, Salcedo-Amaya AM, Smits AH, Francois KJ, et al. 2013. H2A.Z/H2B.Z. double-variant nucleosomes inhabit the AT-rich promoter regions of the *Plasmodium falciparum* genome. *Mol Microbiol* **87**: 1061–73.
67. Petter M, Selvarajah SA, Lee CC, Chin WH, et al. 2013. H2A.Z. and H2B.Z. double-variant nucleosomes define intergenic regions and dynamically occupy var gene promoters in the malaria parasite *Plasmodium falciparum*. *Mol Microbiol* **87**: 1167–82.
68. Siegel TN, Hekstra DR, Kemp LE, Figueiredo LM, et al. 2009. Four histone variants mark the boundaries of polycistronic transcription units in *Trypanosoma brucei*. *Genes Dev* **23**: 1063–76.
69. Cremer T, Kreth G, Koester H, Fink RH, et al. 2000. Chromosome territories, interchromatin domain compartment, and nuclear matrix: an integrated view of the functional nuclear architecture. *Crit Rev Eukaryot Gene Expr* **10**: 179–212.
70. Misteli T. 2007. Beyond the sequence: cellular organization of genome function. *Cell* **128**: 787–800.
71. Takizawa T, Meaburn KJ, Misteli T. 2008. The meaning of gene positioning. *Cell* **135**: 9–13.
72. Freitas-Junior LH, Bottius E, Pirrit LA, Deitsch KW, et al. 2000. Frequent ectopic recombination of virulence factor genes in telomeric chromosome clusters of *P. falciparum*. *Nature* **407**: 1018–22.
73. Ralph SA, Scheidig-Benatar C, Scherf A. 2005. Antigenic variation in *Plasmodium falciparum* is associated with movement of var loci between subnuclear locations. *Proc Natl Acad Sci USA* **102**: 5414–9.
74. Mancio-Silva L, Zhang Q, Scheidig-Benatar C, Scherf A. 2010. Clustering of dispersed ribosomal DNA and its role in gene regulation and chromosome-end associations in malaria parasites. *Proc Natl Acad Sci USA* **107**: 15117–22.
75. Weiner A, Dahan-Pasternak N, Shimoni E, Shinder V, et al. 2011. 3D nuclear architecture reveals coupled cell cycle dynamics of chromatin and nuclear pores in the malaria parasite *Plasmodium falciparum*. *Cell Microbiol* **13**: 967–77.
76. Fullwood MJ, Liu MH, Pan YF, Liu J, et al. 2009. An oestrogen-receptor-alpha-bound human chromatin interactome. *Nature* **462**: 58–64.
77. Guelen L, Pagie L, Brassat E, Meuleman W, et al. 2008. Domain organization of human chromosomes revealed by mapping of nuclear lamina interactions. *Nature* **453**: 948–51.
78. van Koningsbruggen S, Gierlinski M, Schofield P, Martin D, et al. 2010. High-resolution whole-genome sequencing reveals that specific chromatin domains from most human chromosomes associate with nucleoli. *Mol Biol Cell* **21**: 3735–48.
79. Vogel MJ, Peric-Hupkes D, van Steensel B. 2007. Detection of in vivo protein-DNA interactions using DamID in mammalian cells. *Nat Protoc* **2**: 1467–78.
80. Zhao Z, Tavoosidana G, Sjolinder M, Gondor A, et al. 2006. Circular chromosome conformation capture (4C) uncovers extensive networks of epigenetically regulated intra- and interchromosomal interactions. *Nat Genet* **38**: 1341–7.
81. van Steensel B, Dekker J. 2010. Genomics tools for unraveling chromosome architecture. *Nat Biotechnol* **28**: 1089–95.
82. Nora EP, Lajoie BR, Schulz EG, Giorgetti L, et al. 2012. Spatial partitioning of the regulatory landscape of the X-inactivation centre. *Nature* **485**: 381–5.
83. Sofueva S, Yaffe E, Chan WC, Georgopoulou D, et al. 2013. Cohesin-mediated interactions organize chromosomal domain architecture. *EMBO J* **32**: 3119–29.
84. Ferraiuolo MA, Rousseau M, Miyamoto C, Shenker S, et al. 2010. The three-dimensional architecture of Hox cluster silencing. *Nucleic Acids Res* **38**: 7472–84.
85. Rousseau M, Crutchley JL, Miura H, Suderman M, et al. 2014. Hox in motion: tracking HoxA cluster conformation during differentiation. *Nucleic Acids Res* **42**: 1524–40.
86. Li G, Ruan X, Auerbach RK, Sandhu KS, et al. 2012. Extensive promoter-centered chromatin interactions provide a topological basis for transcription regulation. *Cell* **148**: 84–98.
87. Shen Y, Yue F, McCleary DF, Ye Z, et al. 2012. A map of the cis-regulatory sequences in the mouse genome. *Nature* **488**: 116–20.
88. Tanizawa H, Iwasaki O, Tanaka A, Capizzi JR, et al. 2010. Mapping of long-range associations throughout the fission yeast genome reveals global genome organization linked to transcriptional regulation. *Nucleic Acids Res* **38**: 8164–77.
89. Magklara A, Yen A, Colquitt BM, Clowney EJ, et al. 2011. An epigenetic signature for monoallelic olfactory receptor expression. *Cell* **145**: 555–70.
90. Lyons DB, Allen WE, Goh T, Tsai L, et al. 2013. An epigenetic trap stabilizes singular olfactory receptor expression. *Cell* **154**: 325–36.
91. Brancucci NM, Bertschi NL, Zhu L, Niederwieser I, et al. 2014. Heterochromatin protein 1 secures survival and transmission of malaria parasites. *Cell Host Microbe* **16**: 165–76.
92. Coleman BI, Skillman KM, Jiang RH, Childs LM, et al. 2014. A *Plasmodium falciparum* histone deacetylase regulates antigenic variation and gametocyte conversion. *Cell Host Microbe* **16**: 177–86.
93. Le Roch KG, Zhou Y, Blair PL, Grainger M, et al. 2003. Discovery of gene function by expression profiling of the malaria parasite life cycle. *Science* **301**: 1503–8.
94. Otto TD, Wilinski D, Assefa S, Keane TM, et al. 2010. New insights into the blood-stage transcriptome of *Plasmodium falciparum* using RNA-Seq. *Mol Microbiol* **76**: 12–24.
95. Voss TS, Healer J, Marty AJ, Duffy MF, et al. 2006. A var gene promoter controls allelic exclusion of virulence genes in *Plasmodium falciparum* malaria. *Nature* **439**: 1004–8.
96. Dahan-Pasternak N, Nasereddin A, Kolevzon N, Pe'er M, et al. 2013. PfSec13 is an unusual chromatin-associated nucleoporin of *Plasmodium falciparum* that is essential for parasite proliferation in human erythrocytes. *J Cell Sci* **126**: 3055–69.
97. Umbarger MA, Toro E, Wright MA, Porreca GJ, et al. 2011. The three-dimensional architecture of a bacterial genome and its alteration by genetic perturbation. *Mol Cell* **44**: 252–64.
98. Gomez-Diaz E, Corces VG. 2014. Architectural proteins: regulators of 3D genome organization in cell fate. *Trends Cell Biol* **24**: 703–11.
99. Ghorbal M, Gorman M, Macpherson CR, Martins RM, et al. 2014. Genome editing in the human malaria parasite *Plasmodium falciparum* using the CRISPR-Cas9 system. *Nat Biotechnol* **32**: 819–21.
100. Zhang C, Xiao B, Jiang Y, Zhao Y, et al. 2014. Efficient editing of malaria parasite genome using the CRISPR/Cas9 system. *mBio* **5**: e01414–14.
101. Wagner JC, Platt RJ, Goldfless SJ, Zhang F, et al. 2014. Efficient CRISPR-Cas9-mediated genome editing in *Plasmodium falciparum*. *Nat Methods* **11**: 915–8.
102. Bozdech Z, Mok S, Hu G, Imwong M, et al. 2008. The transcriptome of *Plasmodium vivax* reveals divergence and diversity of transcriptional regulation in malaria parasites. *Proc Natl Acad Sci USA* **105**: 16290–5.
103. Fernandez-Becerra C, Pein O, de Oliveira TR, Yamamoto MM, et al. 2005. Variant proteins of *Plasmodium vivax* are not clonally expressed in natural infections. *Mol Microbiol* **58**: 648–58.
104. Le Roch KG, Johnson JR, Florens L, Zhou Y, et al. 2004. Global analysis of transcript and protein levels across the *Plasmodium falciparum* life cycle. *Genome Res* **14**: 2308–18.
105. Bernstein BE, Kamal M, Lindblad-Toh K, Bekiranov S, et al. 2005. Genomic maps and comparative analysis of histone modifications in human and mouse. *Cell* **120**: 169–81.

106. Kim TH, Barrera LO, Zheng M, Qu C, et al. 2005. A high-resolution map of active promoters in the human genome. *Nature* **436**: 876–80.
107. Wang Z, Zang C, Rosenfeld JA, Schones DE, et al. 2008. Combinatorial patterns of histone acetylations and methylations in the human genome. *Nat Genet* **40**: 897–903.
108. Barski A, Cuddapah S, Cui K, Roh TY, et al. 2007. High-resolution profiling of histone methylations in the human genome. *Cell* **129**: 823–37.
109. Nishida H, Suzuki T, Kondo S, Miura H, et al. 2006. Histone H3 acetylated at lysine 9 in promoter is associated with low nucleosome density in the vicinity of transcription start site in human cell. *Chromosome Res* **14**: 203–11.
110. Mikkelsen TS, Ku M, Jaffe DB, Issac B, et al. 2007. Genome-wide maps of chromatin state in pluripotent and lineage-committed cells. *Nature* **448**: 553–60.
111. Lachner M, Sengupta R, Schotta G, Jenuwein T. 2004. Trilogies of histone lysine methylation as epigenetic landmarks of the eukaryotic genome. *Cold Spring Harb Symp Quant Biol* **69**: 209–18.
112. Chantalat S, Depaux A, Hery P, Barral S, et al. 2011. Histone H3 trimethylation at lysine 36 is associated with constitutive and facultative heterochromatin. *Genome Res* **21**: 1426–37.
113. Zlatanova J, Thakar A. 2008. H2A.Z: view from the top. *Structure* **16**: 166–79.
114. Talbert PB, Henikoff S. 2010. Histone variants – ancient wrap artists of the epigenome. *Nat Rev Mol Cell Biol* **11**: 264–75.
115. Bannister LH, Margos G, Hopkins JM. 2005. Making a home for *Plasmodium* post-genomics: ultrastructural organization of the blood stages. In: Sherman IW, ed; *Molecular Approaches to Malaria*. Washington DC: ASM Press. p 24–49.
116. Hoeijmakers WA, Flueck C, Francoijs KJ, Smits AH, et al. 2012. *Plasmodium falciparum* centromeres display a unique epigenetic makeup and cluster prior to and during schizogony. *Cell Microbiol* **14**: 1391–401.
117. Li H, Durbin R. 2010. Fast and accurate long-read alignment with Burrows–Wheeler transform. *Bioinformatics* **26**: 589–95.